Journal of Applied Polymer Science

Packaging technology for improving shelf-life of fruits based on a nanoporous–crystalline polymer

Paola Rizzo,[1,2] **Antonietta Cozzolino**,[2] **Alexandra R. Albunia**,[1,3] **Angelo Maria Giuffrè**,[4] **Vincenzo Sicari**,[4] **Luciano Di Maio**,[5] **Christophe Daniel**,[1,2] **Vincenzo Venditto**,[2] **Maurizio Galimberti**,[1,6] **Giuseppe Mensitieri**,[7] **Gaetano Guerra**[1,2]

[1]NanoActive Film s.r.l, Fisciano, Italy
[2]Department of Chemistry and Biology and INSTM Research Unit, University of Salerno, Via Giovanni Paolo II 132, Fisciano Salerno 84084, Italy
[3]Borealis Polyolefine GmbH, St.-Peter-Strasse 25, Linz 4021, Austria
[4]Department of Agraria, University "Mediterranea" of Reggio Calabria, Salita Melissari Reggio Calabria 89124, Italy
[5]Department of Industrial Engineering, University of Salerno, Via Giovanni Paolo II 132, Fisciano SA 84084, Italy
[6]Department of Chemistry, Materials, and Chemical Engineering, Politecnico di Milano, via Mancinelli 7, Milan 20131, Italy
[7]Department of Materials and Production Engineering, University of Naples Federico II, P.le Tecchio 80, Naples 80125, Italy
Correspondence to: Paola Rizzo (E-mail: prizzo@unisa.it)

ABSTRACT: The ability of films with an active layer of nanoporous–crystalline syndiotactic polystyrene (s-PS) to prolong shelf-life, not only of climacteric but also of non-climacteric fruits, is discussed. Studies on oxygen and carbon dioxide concentrations in the environment of packaged fruits as well as in s-PS active layers have been combined. Reported results indicate that prolonged shelf-life can be associated with large increases and decreases of carbon dioxide and oxygen concentrations inside the package, respectively. These data are consistent with a higher barrier offered to both gases by nanoporous–crystalline s-PS layers. This barrier phenomenon is due to reduction of gas diffusivity typical of nanoporous–crystalline polymer films, which is further enhanced by orientation, parallel to the film plane, of crystalline planes of closely packed s-PS helices. © 2018 Wiley Periodicals, Inc. J. Appl. Polym. Sci. **2018**, *135*, 46256.

KEYWORDS: films; nanoporous crystalline polymer; packaging; polystyrene

Received 20 October 2017; accepted 23 December 2017
DOI: 10.1002/app.46256

INTRODUCTION

Food packaging continues to evolve in response to the advancement of material science and technology, as well as the changing consumers' demand towards preserved, fresh, tasty and convenient food products with prolonged shelf-life and controlled quality.[1–4]

In particular active packaging includes oxygen scavengers,[5,6] ethylene scavengers, flavor and odor absorber/releaser, antimicrobial, and antioxidant into packaging systems[7] with the aim of extending food products quality and shelf-life.[8–11]

The ability to prolong shelf-life of fruit and vegetables, by active films with a nanoporous crystalline s-PS layer, has been described in an international patent[12] as well as in a recent article in which is shown the ability of active s-PS nanoporous–crystalline layer to prolong shelf-life of non-climacteric fruits, like oranges.[13]

Nanoporous–crystalline forms have been discovered for two industrially relevant polymers: syndiotactic polystyrene (s-PS)[14–18] and poly(2,6-dimethyl-1,4-phenylene)oxide (shortly named as PPO).[19]

As for s-PS the δ nanoporous crystalline form presents, inside the crystalline lattice, isolated cavities having a volume close to 0.125 nm^3, whereas the ε nanoporous crystalline form presents channels with a diameter of ≈0.5 nm.[20] It is well known the ability of polymeric nanoporous forms to absorb in their crystalline cavities low-molecular-mass molecules, thus forming stable host/guest co-crystalline phases.[20–22]

Co-crystalline phases, being unstable due to guest release in few minutes or hours, can be also formed with molecules being gaseous at room temperature, like carbon dioxide,[23] ethylene,[24] and even hydrogen.[25,26] Co-crystalline phases, with carvacrol (a relevant natural antimicrobial molecule) being prevailingly (more than 90%) guest of the cocrystalline phase have been prepared, even for high carvacrol content (up to 10–11 wt %). The location of most antimicrobial molecules in the crystalline phase assures a decrease of desorption diffusivity of two to three orders and hence long-term antimicrobial release.[27]

Molecular transport mechanisms determining prolonged shelf-life of fruit and vegetables, as observed for films based on nanoporous–crystalline s-PS, have not been fully clarified.

In particular, the high solubility of ethylene in crystalline cavities of s-PS films[24] has suggested that prolonged shelf life could be associated with reduction of ethylene concentration in fruit packaging. In fact, it is well known that ethylene is the hormone for ripening of climacteric fruits and vegetables.[28]

Recent studies have shown the ability of films including a s-PS nanoporous-crystalline layer to prolong shelf-life also of non-climacteric fruits, like oranges[13] indicating that an alternative or at least an additional molecular mechanism has to be involved. Studies on packaging of oranges indicate that prolonged shelf-life is associated with definitely increased carbon dioxide and decreased oxygen concentrations in the environment of packaged fruits.

In this article, studies on oxygen and carbon dioxide concentrations in the environment of packaged non-climacteric fruits as well in s-PS nanoporous-crystalline layers have been combined. The aim is to understand transport phenomena in active s-PS packaging films that control O_2 and CO_2 concentration in the fruit environment, which in turn are determinant in fruit and vegetable preservation.

EXPERIMENTAL

Materials

Three layer PP/s–PS/PP films with overall thickness of nearly 40 μm (14/12/14) were co-extruded by blown process. The external layers of PP/s–PS/PP films are made by isotactic polypropylene (i-PP), MOPLEN PP310D produced by LyondellBasell, (≈14 μm thick), and the inner layer by syndiotactic polystyrene (s-PS) Questra 101 produced by Dow Chemical Company, with thickness of approximately 12 μm. They were obtained by a bubble extrusion process using a melt temperature of 190 °C for the i-PP and 290 °C for s-PS. The bubble was obtained using a BUR (Blow up ratio) equal to 2.5 and a DR (draw ratio) equal to 8. In these three-layer films, the layer based on s-PS, after extrusion, was completely amorphous. The activation process involves film treatment with methylacetate.[12]

Biaxially Oriented Isotactic Polypropylene films (PP) (20 μm thick), exhibit α crystalline form, a degree of crystallinity close to 45% and a degree of uniplanar orientation evaluated on the azimuthal scan of the 040 reflection close to 0.8.

Biaxially oriented poly(ethylene terephthalate) (PET) films (12 μm thick), present a degree of crystallinity close to 40%, a degree of uniplanar orientation evaluated on the azimuthal scan of the 100 reflection close to 0.8.

Plastic bags under air atmosphere were sealed by a Multivac Vacuum machine model 550/S (GAS - Univac Group S.r.l., Lavezzini division, Fiorenzuola d'Arda, Piacenza, Italy). Each piece of film, with a rectangular shape, was bent on one of the two long sides and then sealed on the remaining three sides after the introduction of the oranges or the pan containing the raspberries. One septum (15 mm diameter; 2 mm thickness) was applied on the outside of each package, this make possible to do several measurements on the same package. O_2 and CO_2 content was measured in the atmosphere of the package by a PBI Dansensor (Ringsted, Denmark) model Check Point. This instrument is equipped with a needle which is used to pierce the septum and the packaging film before to quantify gases. Results are expressed as % v/v

Oranges Packaging and O_2 and CO_2 Quantification

The oranges (*Citrus sinensis cv* Belladonna) were randomly collected in November 2015 in a farm in the South of Italy. Fruits were carefully placed in a plastic fruit crate and they were quickly brought to the laboratory. After this, oranges were randomly packaged as follows: three fruits were packaged in each bag using two different films, a Activated Nanoactive film and a conventional antifog biaxially oriented PP film. All samples were stored at 6 ± 0.5 °C (80% RH) and headspace gas composition was detected every 15 days. To avoid modifications in the atmosphere due to gas sampling, each package was used for only a single measurement.

Raspberries Packaging and O_2 and CO_2 Quantification

Raspberries (*Rubus idaeus* L., cv Erika) grown in a greenhouse in the Reggio Calabria Province (Italy) were randomly and manually picked on May 27, 2015 at 7.00 AM at the white stage of color development, that is, when fruits showed a faint pink color. At this point raspberries were placed in PET containers (100 g per container) and immediately brought to the laboratory. Three different flexible films were used for packaging: that is, activated nanoactive film, not activated nanoactive film and biaxially oriented PET film. After packaging raspberries were put in the fridge at 1 °C until analysis.

Daily, three packages for each used film were taken and gases were detected from each package. Results are the mean ± SD of the three measurements. O_2 and CO_2 detection was conducted for 7, 12, and 14 days for not activated nanoactive, PET, and activated nanoactive films, respectively, that is, until fruits were found to be swollen or mold appeared.

Characterization Techniques

Oxygen and carbon dioxide sorption in polymer films were measured by an electronic microbalance, CAHN D200, with a sensitivity equal to 0.1 mg, equipped with a controlled environment cell. Gas sorption tests were conducted at sub-atmospheric pressures (from 80 to 760 Torr). The head of the balance was kept at a constant temperature (35 °C) while the temperature of the sample pan was controlled by means of a water jacket. The microbalance was connected through service lines to the rest of the apparatus equipped with a pressure transducer, a 'Pirani' vacuometer, a glass flask and connected to the gas cylinder and a turbomolecular vacuum pump.

Before performing sorption tests, the samples were desiccated into the microbalance at 60 °C under vacuum until the attainment of a constant weight. Consecutive sorption–desorption cycles were performed at 35 °C. Pressure was monitored by means of a MKS Baratron 121 pressure transducer with a full scale of 1000 Torr, a sensitivity of 0.1 Torr and an accuracy of ±0.5% of the reading.

Fourier transform infrared (FTIR) spectra were obtained at a resolution of 2.0 cm^{-1} with a Vertex 70 Bruker spectrometer. A total of 32 scans were signal averaged to reduce the noise.

The infrared based degree of crystallinity of the activated s-PS layer was evaluated according to $K = l/l'$ $(1 - Xc)$ where K is the subtraction coefficient, l and l' are the thickness of the activated layer and of the amorphous s-PS reference layer as described in literature.[29]

Wide-angle X-ray diffraction patterns were obtained by an automatic Bruker D8 Advance powder diffractometer (CuKa radiation) operating in the θ/2θ Bragg–Brentano geometry using specimen holders 2 mm thick and in transmission by a D8 QUEST Bruker diffractometer (CuKa radiation) sending the X-ray beam parallel to the film surface.

The degree of uniplanar orientation of a crystal plane exhibiting *hkl* Miller indexes (f_{hkl}), with respect to the film plane, has been formalized on a quantitative numerical basis using Hermans' orientation function[30,31]:

$$f_{hkl} = (3\overline{\cos^2 x_{hkl}} - 1)/2 \quad (1)$$

by assuming $\overline{\cos^2 x_{hkl}}$ as the average cosine squared values of the angle, x_{hkl}, between the normal to the film surface and the normal to the (hkl) crystallographic plane.

If the direction normal to the *hkl* plane is unique (i.e., there are no other equivalent directions in the crystal), f_{hkl} is equal to +1 or −0.5 when the (hkl) crystallographic planes of all crystallites are perfectly parallel or perpendicular to the film plane, respectively. For the case of random orientation f_{hkl} is equal to zero.

The quantity $\overline{\cos^2 x_{hkl}}$ has been experimentally evaluated as:

$$\overline{\cos^2 \chi_{hkl}} = \overline{\cos^2 \chi_{hkl}} = \frac{\int_0^{\pi/2} I(\chi_{hkl}) \cos^2 \chi_{hkl} \sin \chi_{hkl} d\chi_{hkl}}{\int_0^{\pi/2} I(\chi_{hkl}) \sin \chi_{hkl} d\chi_{hkl}} \quad (2)$$

where $I(\chi_{hkl})$ is the intensity distribution of a (hkl) diffraction on the Debye ring and χ_{hkl} are the azimuthal angles measured from the horizontal line of the pattern of Figure 2(c).

Theoretical Background

Postharvest horticultural products are perishable respiring tissues. An important aspect of postharvest physiology, in presence of molecular oxygen, is aerobic respiration consisting in the oxidation of organic substrates that produces, besides energy and other molecules, water and carbon dioxide. Different products are characterized by different respiration rates and by a different value of the Respiratory Quotient (RQ) (i.e., the ratio of volume of carbon dioxide released to the volume of oxygen consumed), that ranges from 0.7 to 1.3 and could depend on the relative pressures of oxygen and carbon dioxide.[32] When oxygen concentration is below a threshold value (the so-called extinction point) respiration process changes from aerobic to anaerobic. Non-climateric fruits (like oranges and raspberries) are characterized by the fact that ripening is not associated with marked respiratory rise and with increase of ethylene production.

Based on the chemical reactions occurring during aerobic respiration, it is evident that the respiration rate decreases when the concentration of CO_2 increases and that of O_2 decreases in the environment surrounding the fruit product, thus prolonging its storage life. However, excessively low values of oxygen concentration should be avoided otherwise an unacceptable increase of anaerobic respiration occurs with associated damage of plant tissue.

In a passive-modified atmosphere packaging, several factors determine the time evolution of carbon dioxide and oxygen concentration in the headspace of a packaging containing non-climateric fruits. Among them, the most relevant are the initial composition of the headspace atmosphere, the transport properties of packaging film, by the surface to volume ratio of the package, by the effect of gas concentration on respiration rate and by the value of RQ. Possibly, the system reaches a steady state (i.e., a condition of constant concentration of both gases in the headspace) when the inflow of oxygen and the outflow of carbon dioxide exactly balance the relative consumption and production determined by the respiration.

In particular, at steady state the following relationships hold[32]:

$$\frac{P_{O_2} A}{L} = \frac{R_{O_2} W}{\left(p_{out}^{O_2} - p_{in}^{O_2}\right)} \quad (3)$$

$$\frac{P_{CO_2} A}{L} = \frac{RQ\, R_{O_2} W}{\left(p_{in}^{CO_2} - p_{out}^{CO_2}\right)} \quad (4)$$

where P_{O_2} and P_{CO_2} are, respectively, the permeation coefficient to oxygen and carbon dioxide that are related to the flux of oxygen (Q_{O_2}) and carbon dioxide (Q_{CO_2}) through the polymer by the following expressions:

$$Q_{O_2} = \frac{P_{O_2} A}{L}\left(p_{out}^{O_2} - p_{in}^{O_2}\right) \quad (5)$$

$$Q_{CO_2} = \frac{P_{CO_2} A}{L}\left(p_{in}^{CO_2} - p_{out}^{CO_2}\right) \quad (6)$$

In the previous expressions, W is the weight of fruit, A is the area of packaging film exposed to gas flux, L is the thickness of the film, and R_{O_2} is the rate of oxygen consumption in terms of volume of oxygen consumed per unit time and unit weight of fruit and is, in general, a function of both partial pressure of oxygen and of carbon dioxide in the head space of packaging. Finally, $p_{out}^{O_2}$, $p_{out}^{CO_2}$, $p_{in}^{CO_2}$, and $p_{in}^{O_2}$ represent, respectively, the partial pressure of oxygen and carbon dioxide outside and inside the package. It is worth noting that the packaged fruit does not necessarily reach the steady state conditions described by previous expressions during its commercial life. In fact, the system can be in a transient regime during the entire shelf life.

Optimal headspace atmospheres that guarantee the longest shelf life (in terms of gas volumetric concentration) are, for raspberries, 5–10% of oxygen and 15–19% of carbon dioxide while, for oranges, 5–10% of oxygen and 0–5% of carbon dioxide.[32]

RESULTS AND DISCUSSION

Structural and Morphological Characterization of Three-Layer PP/s–PS/PP Films

The present study mainly compares three-layer PP/s–PS/PP films, which have been obtained by the co-extrusion process described in the experimental section. The only difference between active and reference films is the subsequent activation by a sorption/desorption procedure at room temperature with

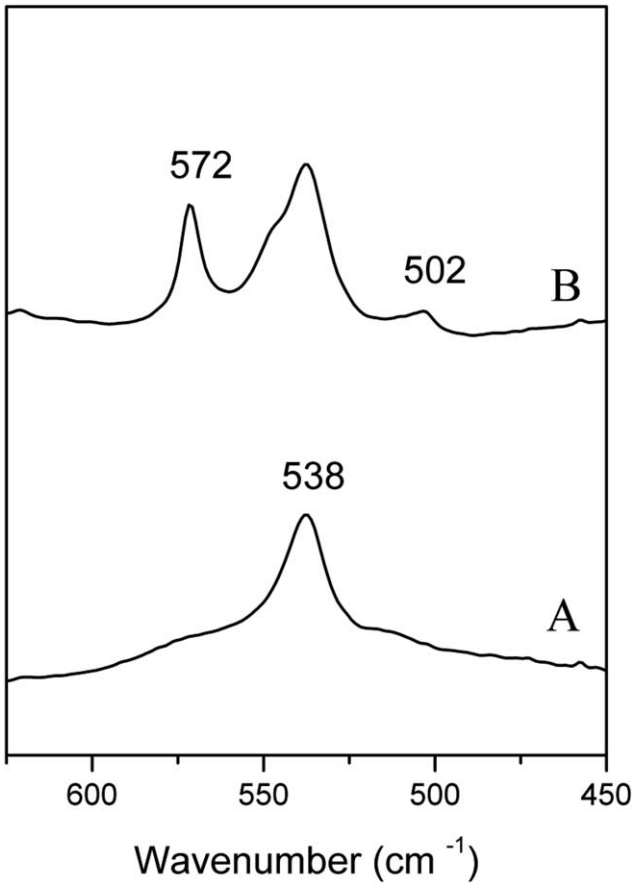

Figure 1. FTIR spectra in the spectral range 450–625 cm^{-1} of the intermediate s-PS layer before (a) and after sorption–desorption of methylacetate (b).

an eco-friendly guest (methylacetate), as also taught by the above cited patent.[12]

In Figure 1 are reported the FTIR spectra in the spectral range 450–625 cm^{-1} of the intermediate s-PS layer before (A) and after sorption–desorption of methylacetate (B).

The FTIR spectrum of the s-PS layer after sorption–desorption of methylacetate (B) presents two peaks at 572 and 502 cm^{-1} which were initially absent (curve A). These peaks which are typical of the s-PS s(2/1)2 ordered helical conformation[33] indicates that crystallization of the s-PS layer has been achieved. The infrared degree of crystallinity is 25% as evaluated according to literature.[29]

X-ray diffraction patterns show that the intermediate s-PS layer of the reference film is fully amorphous [Figure 2(a)] while the same film, after activation by methylacetate, exhibits a disordered nanoporous crystalline phase,[17] as shown by the presence of broad 010 diffraction peak at $2\vartheta = 9.3°$ [Figure 2(b)]. The high intensity of the 010 peak clearly suggests the presence of a preferential orientation of the 010 plane (and hence of the *ac* plane) parallel to the film plane.[34] The occurrence of the uniplanar $a_{//}c_{//}$orientation is clearly confirmed by the 2D WAXD pattern, collected by having the X-ray beam parallel to the film plane [Figure 2(c)], where the 010 is centered on the equator. A degree of uniplanar orientation close to 0.7 can be evaluated on the basis of an azimuthal scan of the 010 reflection of Figure 2(c).

Moreover, the half-height width of the 010 reflection centered at $2\vartheta \approx 9.3°$ allows evaluating a correlation length of nearly 3 nm, indicating the presence of few (on average three) piled high-density and low-energy *a–c* planes, constituted by alternated enantiomorphous s(2/1)2 helices, as shown by the molecular model of Figure 3(a). A schematic presentation of this uniplanar $a_{//}c_{//}$orientation, for the activated s-PS layer, is shown in Figure 3.

O_2 and CO_2 Concentrations inside Fruit Packages

O_2 and CO_2 concentrations inside packages of oranges and raspberries, with different kinds of polymer films, are plotted versus time in Figure 4(a, b), respectively. For both kinds of non-climacteric fruits, the behavior of active and reference films is largely different. In fact, in the environment of fruits packaged by the three layer active film, exhibiting a nanoporous

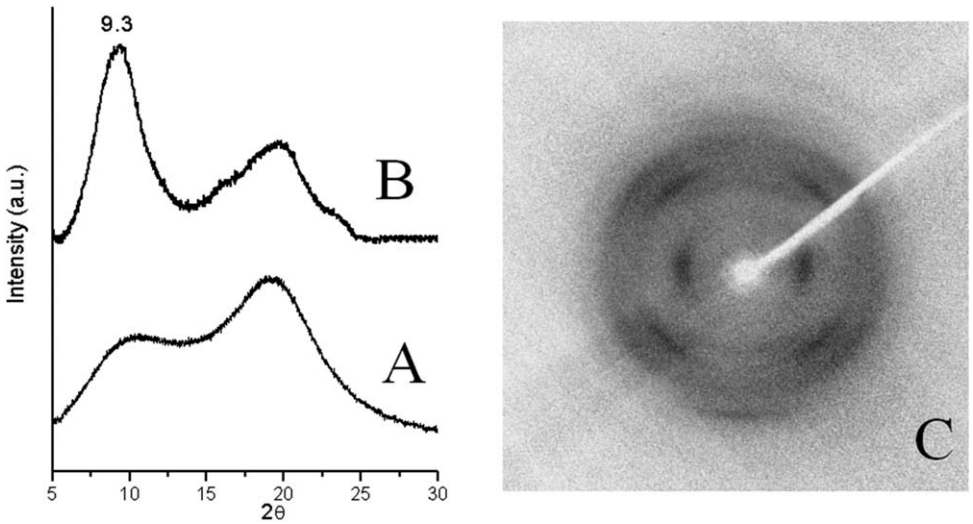

Figure 2. X-ray diffraction patterns (CuKα) of intermediate s-PS layers of PP/s–PS/PP films: before (a) and after activation by methylacetate (b,c). Patterns A and B are taken by an automatic powder diffractometer while the two-dimensional pattern C is taken by having the X-ray beam parallel to the film plane.

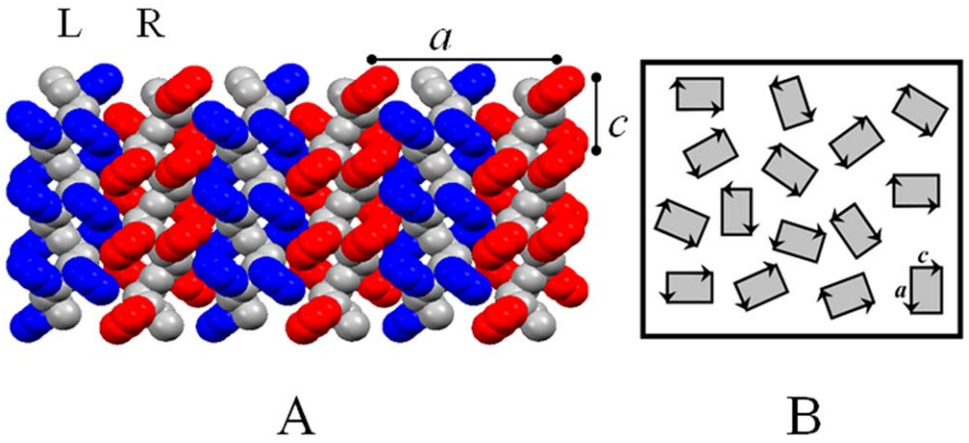

Figure 3. (a) Lateral view of the high density and low-energy *a–c* molecular layer of s(2/1)2 parallel helices of s-PS, i.e., a structural feature which is common to δ nanoporous forms and to corresponding co-crystalline forms. The short interchain distance is achieved by alternating enantiomorphous right-handed (R) and left-handed (L) helices. Gas diffusivity through these molecular planes is of course low. According to the WAXD analysis of Figure 2 these molecular planes are preferentially parallel to the s-PS macroscopic layers, as schematically shown in (b). [Color figure can be viewed at wileyonlinelibrary.com]

crystalline s-PS layer, O_2, and CO_2 concentrations markedly decrease and increase, respectively, with packaging time, (red-continuous curves in Figure 4). Instead, in the environment of fruits packaged by reference (non-activated) three-layer films, exhibiting an amorphous s-PS layer changes of O_2 and CO_2 concentrations with packaging time are less pronounced. It is likely that, already in the very first few days, these systems attain the steady state regime described by eqs. (3–6).

For the case of oranges [Figure 4(a)] and of raspberries [Figure 4(b)], data relative to gas concentrations in standard PP and PET packaging have been also reported. It is apparent that PP and PET packaging behave in a way more similar to non-activated three-layer films, with smaller changes in O_2 and CO_2 concentrations.

The large decreases and increases of O_2 and CO_2 concentrations observed for the activated film are consistent with a higher barrier offered by the multilayer film containing a δ form s-PS layer. It is worth noting that, for experiments performed using such a film, the entire process, including respiration reactions and mass transport through the multilayer film, apparently reaches the steady state only at the end of the tests, thus implying that the monitoring of concentration of oxygen and carbon dioxide mostly occurs within the timeframe of non-steady state (transient) regime. In the following, we propose an interpretation of the observed results on the basis of the peculiarities of sorption and mass transport behavior of oxygen and carbon dioxide in δ form s-PS.

Solubility and Diffusivity of O_2 and CO_2 in Nanoporous-Crystalline Polymer Films

Sorption isotherms of O_2 and CO_2 in different PS films are compared in Figure 5. The reported data refer to a nanoporous–crystalline s-PS phase and to a fully amorphous a-PS film.[35] It is immediately apparent that both O_2 and CO_2 exhibit low solubility in fully amorphous polystyrene films while solubility of both molecules is much higher in the nanoporous–crystalline phase. In particular, CO_2 solubility reaches (for pressures close to 700 torr) values as high as 18 cm^3 (STP)/cm^3 of polymer crystalline phase. For instance, for an internal atmosphere containing 20 wt % of CO_2 at a total pressure of 1 atm, corresponding to a partial pressure of 150 torr, the CO_2 content in the polymer film is close to 4 cm^3 (STP)/cm^3 of polymer crystalline phase.

The high solubility of carbon dioxide in nanoporous crystalline forms of s-PS has been also pointed out by FTIR analyses.[23] In particular, as described in details in Ref. 23, the use of polarized infrared radiation and of axially oriented films has allowed to establish that most of CO_2 molecules are absorbed as guest of the crystalline cavities. Particularly informative are FTIR spectra of the polymer films at the end of the packaging experiments, in regions of absorbance bands of water and carbon dioxide (Figure 6), that is, of main compounds released by fruits and vegetables. H_2O and CO_2 bands are negligible for FTIR spectra collected for amorphous s-PS as well as for commercial PP and PET films, indicating that their H_2O and CO_2 solubility is negligible. The FTIR spectrum of the active film (in particular, of the intermediate nanoporous–crystalline s-PS layer), reported as a thick red curve in Figure 6 shows an intense CO_2 band, which well agrees with the high CO_2 solubility shown by measurements of Figure 5.

It is also worth comparing the FTIR spectrum, at the end of the packaging experiment, of a commercial active film, prepared by compression molding of a commercial masterbatch, whose ethylene and CO_2 absorption is based on mesoporous silica (thin black curve in Figure 6). The presence of an intense and broad band centered at 3400 cm^{-1} clearly indicates that the polymer film with silica beside CO_2 also absorbs large amount of water. This, of course, constitutes a relevant advantage of s-PS-based active films that avoid water removal from packaged fruit and hence moisture loss from fruit and vegetables.

The spectra of Figure 6 also show that the absorbance band of ν_3 CO_2 antisymmetric stretching mode for molecules absorbed in both packaging active films is red-shifted (2334 and 2338 cm^{-1}) from the gas-phase value of 2349 cm^{-1}, as a result of interactions with adsorption sites.[36] Moreover, the CO_2 peak

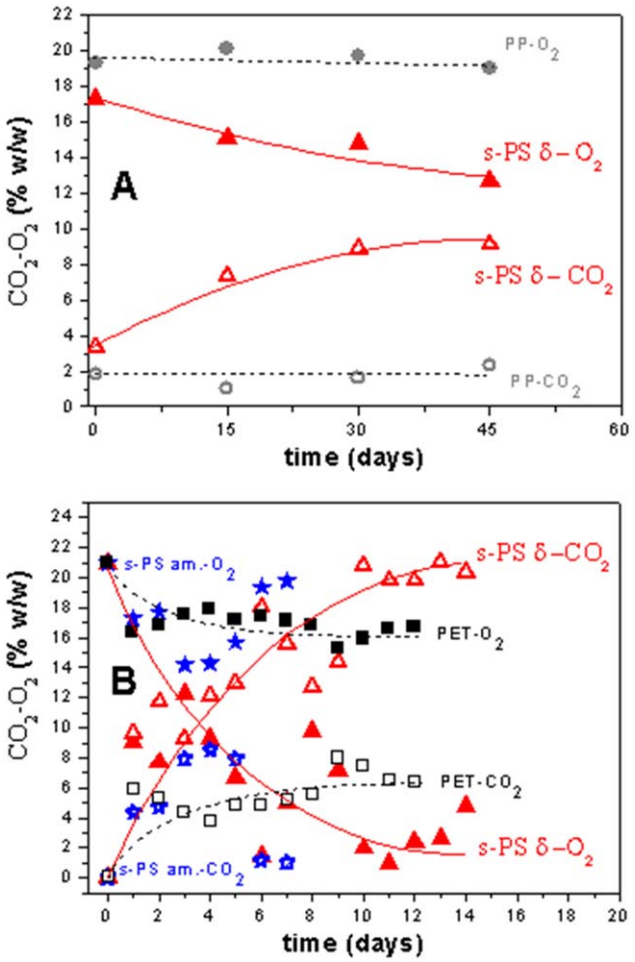

Figure 4. O_2 (filled symbols) and CO_2 (empty symbols) concentrations inside packages of oranges (a) and raspberries (b), for reference (star) and active (triangle) three-layer PP/s–PS/PP films, plotted versus time. O_2 and CO_2 concentrations are also reported for standard packaging of PP (circle) and PET(square), in (a) and in (b), respectively. [Color figure can be viewed at wileyonlinelibrary.com]

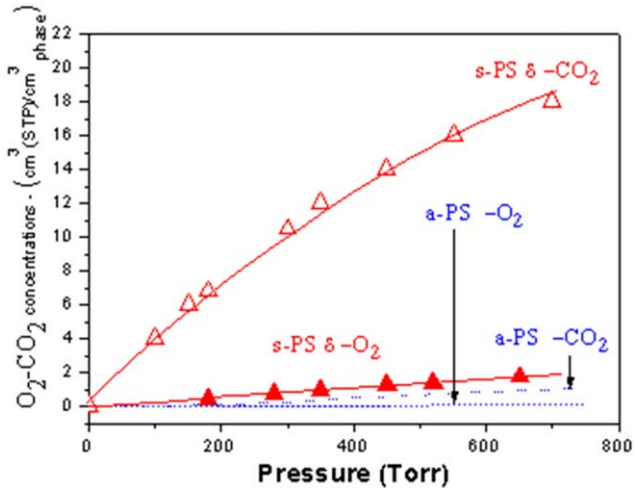

Figure 5. Sorption isotherms at 35 °C of O_2 (red filled triangles) and CO_2 (red empty triangles) in nanoporous–crystalline s-PS phase (red continuous lines) and in amorphous a-PS films (blue dashed lines). [Color figure can be viewed at wileyonlinelibrary.com]

is definitely narrower for the s-PS active film than for the silica based active film, with half-height-width reducing from 12 to 2 cm^{-1}. This phenomenon is determined by the inclusion of CO_2 molecules in the cavities of nanoporous crystalline phases of s-PS, which has been demonstrated by X-ray diffraction patterns as well as by polarized FTIR spectra of axially stretched films.[23] In fact, as modelled in detail in,[37] CO_2 molecules are definitely more mobile inside the crystalline cavity, than in the free-volume of the corresponding amorphous phase, thus determining the observed narrower absorbance FTIR peaks, more similar to sharp peaks of gaseous CO_2.

Differences in diffusivities of O_2 and CO_2 in amorphous and nanoporous-crystalline phases of s-PS are also relevant for the gas concentrations in fruit packaging. Diffusivities of both molecules are definitely higher in the fully amorphous polystyrene film (i.e., at 35 °C, 1.2×10^{-7} and 0.78×10^{-7} cm^2/s for O_2 and CO_2, respectively) than in nanoporous crystalline phases (again at 35 °C, 6.3×10^{-9} and 0.62×10^{-9} cm^2/s for O_2 and CO_2, respectively).[35] Molecular simulations suggest that lower gas diffusivities for the nanoporous–crystalline phase are due to a diffusion mechanism that proceeds by hopping between different crystalline cavities. For some period of time, the penetrant stays in a cavity region. During such a quasi-stationary period, it explores this region but does not move beyond the cavity confines. The quasi-stationary periods are interrupted by quick leaps from one cavity into a neighboring one.[37]

Hence, for nanoporous crystalline phases of s-PS, CO_2 solubility is roughly one order of magnitude higher than O_2 solubility while, on the contrary, CO_2 diffusivity is roughly one order of magnitude lower than O_2 diffusivity. Moreover, when the mass transport and sorption properties of nanoporous crystalline and amorphous phases of s-PS are compared[35] it is evident that, for both gases, we have a much higher solubility and a much lower diffusivity in the crystalline regions, as compared to the amorphous ones.

Based on these results, one would have a steady state permeability of both gases that in a hypothetical totally crystalline phase would be one order of magnitude lower than in the case of a

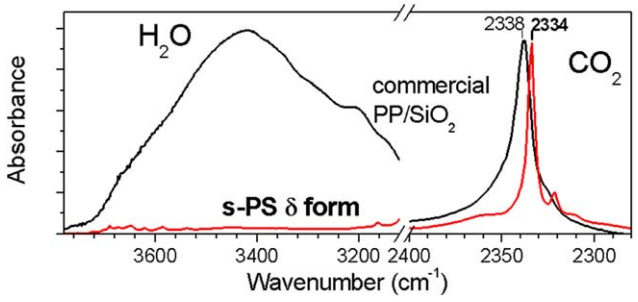

Figure 6. FTIR spectra of polymer films after two weeks of storage of oranges: (black lines) a PP/SiO_2 80/20 commercial masterbatch film; (red lines) an activated s-PS layer. The considered spectral ranges (3800–3100 and 2400–2280 cm^{-1}) include typical absorbance bands of water and carbon dioxide, respectively. [Color figure can be viewed at wileyonlinelibrary.com]

totally amorphous phase. One would then conclude that a semicrystalline s-PS film with a nanoporous crystalline phase would offer a higher barrier to both gases as compared to an amorphous s-PS film since the crystalline domains act as obstacles to permeation. This effect would be rather limited in case of isolated crystallites and of a well-connected amorphous phase and would not justify, taken alone, the relevant differences measured for gas concentration evolution within package headspace between the cases where amorphous s-PS and nanoporous semicrystalline s-PS are used.

It is likely that the striking difference between the two types of multilayer films results from a morphology of the semicrystalline polymer consisting in high aspect ratio crystallites that confine isolated amorphous domains. Thin *ac* layers being parallel to the film plane, as indicated by the WAXD data of Figure 2 and schematically shown in Figure 3(b), could possibly correspond to a morphology that highly increases the effectiveness of nanoporous crystalline domains in obstructing diffusion. In this respect, it is worth citing that molecular dynamic simulations have shown that diffusivity of CO_2 perpendicular to these dense layers is essentially negligible.[37] It is also well established that diffusivity of a chlorinated hydrocarbon is minimum for films exhibiting uniplanar $a_{//}c_{//}$orientation.[38,39] This effect is expected to be much more relevant during transient regimes, since 'dead end' paths would adversely affect the effective rate of diffusion.

In addition, there is a mutual effect of presence of both gases within the crystalline nanocavities that promotes a further decrease of diffusivities within the crystals. Taken together, these arguments provide a reasonable interpretation for the experimental outcomes in terms of evolution of carbon dioxide and oxygen within the package headspace.

It is worth noting that the possibility of changing the morphology of amorphous s-PS by a proper treatment, allowed the attainment of significant differences in the relevant barrier properties of the multilayer film and potentially opens the way to a tailoring of mass transport properties to guarantee the best performance in terms of modified atmosphere composition for each kind of packaged fruit.

CONCLUSIONS

Films with s-PS active layers, exhibiting a nanoporous–crystalline phase, are able to prolong shelf-life not only of climacteric but also of non-climacteric fruits.

Studies inside packages of non-climacteric fruits (oranges and raspberries) show that for three-layer active film, exhibiting a nanoporous–crystalline s-PS layer, O_2, and CO_2 concentrations markedly decrease and increase, respectively, with packaging time. In the same conditions, for reference films (not activated three layer films or biaxially oriented commercial PP and PET films), smaller variations with packaging time of O_2 and CO_2 concentrations are observed.

This behavior is due to a higher barrier to O_2 and CO_2 diffusion, offered by the activated (nanoporous–crystalline) δ form of s-PS layer. These δ form s-PS layers exhibit, for both gases, higher solubility and a much lower diffusivity in the crystalline regions, as compared to the amorphous ones. This reduction of gas diffusivity is enhanced by orientation, parallel to the film plane, of crystalline planes of closely packed s-PS helices.

Increase of CO_2 concentration inside fruit package has also a remarkable positive effect in slowing down the development of molds, due to well-known anti-microbial properties of carbon dioxide.

ACKNOWLEDGMENTS

The authors thank I. Immediata for useful discussions and also acknowledge "Ministero dell'Istruzione, dell'Università e della Ricerca" for financial support.

REFERENCES

1. Mihindukulasuriya, S. D. F.; Lim, L. T. *Food Sci. Technol.* **2014**, *40*, 149.
2. Ramos, M.; Fortunati, E.; Peltzer, M.; Jimenez, A.; Kenny, J. M.; Garrigós, M. C. *Polym. Degrad. Stabil.* **2016**, *132*, 2.
3. Fortunati, E.; Armentano, I.; Zhou, Q.; Iannoni, A.; Saino, E.; Visai, L.; Berglundd, L. A.; Kenny, J. M. *Carbohydr. Polym.* **2012**, *87*, 1596.
4. Fortunati, E.; Luzi, F.; Puglia, D.; Dominici, F.; Santulli, C.; Kenny, J. M.; Torre, L. *Eur. Polym. J.* **2014**, *56*, 77.
5. Scarfato, P.; Avallone, E.; Galdi, M. R.; Di Maio, L.; Incarnato, L. *Polym. Compos.* **2017**, *38*, 981.
6. Di Maio, L.; Scarfato, P.; Galdi, M. R.; Incarnato, L. *J. Appl. Polym. Sci.* **2015**, *41465*, 1.
7. Burgos, N.; Armentano, I.; Fortunati, E.; Dominici, F.; Luzi, F.; Fiori, S.; Cristofaro, F.; Visai, L.; Jiménez1, A.; Kenny, J. M. *Food Bioprocess Technol.* **2017**, *10*, 770.
8. Krepker, M.; Shemesh, R.; Poleg, Y.; Kashi, Y.; Vaxman, A.; Segal, E. *Food Control* **2017**, *76*, 117.
9. Ramos, M.; Jimenez, A.; Peltzer, M.; Garrigos, M. C. *J. Food Eng.* **2012**, *109*, 513.
10. Lavoine, N.; Desloges, I.; Bras, J. *Carbohydr. Polym.* **2014**, *103*, 528.
11. Lopez de Dicastillo, C.; Nerin, C.; Alfaro, P.; Catala, R.; Gavara, R.; Hernandez-Munoz, P. *J. Agric. Food Chem.* **2011**, *59*, 7832.
12. Albunia, A. R.; Bianchi, R.; Maio, L. D.; Galimberti, M.; Guerra, G.; Pantani, R.; Senatore, S. (Nano Active Film S.r.l.). PCT Int. Appl. WO 2012089805, July 05, **2012**.
13. Sicari, V.; Dorato, G.; Giuffrè, A. M.; Rizzo, P.; Albunia, A. R. *J. Food Process. Preserv.* **2017**, *41*, e13168.
14. De Rosa, C.; Guerra, G.; Petraccone, V.; Pirozzi, B. *Macromolecules* **1997**, *30*, 4147.
15. Petraccone, V.; Ruiz de Ballesteros, O.; Tarallo, O.; Rizzo, P.; Guerra, G. *Chem. Mater.* **2008**, *20*, 3663.
16. Tarallo, O.; Petraccone, V.; R. Albunia, A.; Daniel, C.; Guerra, G. *Macromolecules* **2010**, *43*, 8549.
17. Rizzo, P.; Ianniello, G.; Albunia, A. R.; Acocella, M. R.; Guerra, G. *J. Solution Chem.* **2014**, *43*, 158.

18. Acocella, M. R.; Rizzo, P.; Daniel, C.; Tarallo, O.; Guerra, G. *Polymer* **2015**, *63*, 230.
19. Daniel, C.; Longo, S.; Fasano, G.; Vitillo, J. G.; Guerra, G. *Chem. Mater.* **2011**, *23*, 3195.
20. Guerra, G.; Daniel, C.; Rizzo, P.; Tarallo, O. *J. Polym. Sci. Pol. Phys.* **2012**, *50*, 305.
21. Daniel, C.; Antico, P.; Yamaguchi, H.; Kogure, M.; Guerra, G. *Micropor. Mesopor. Mater.* **2016**, *232*, 205.
22. Musto, P.; Rizzo, P.; Guerra, G. *Macromolecules* **2005**, *38*, 6079.
23. Annunziata, L.; Albunia, A. R.; Venditto, V.; Mensitieri, G.; Guerra, G. *Macromolecules* **2006**, *39*, 9166.
24. Albunia, A. R.; Minucci, T.; Guerra, G. *J. Mater. Chem.* **2008**, *18*, 1046.
25. Figueroa-Gerstenmaier, S.; Daniel, C.; Milano, G.; Guerra, G.; Zavorotynska, O.; Vitillo, J. G.; Zecchina, A.; Spoto, G. *Phys. Chem. Chem. Phys.* **2010**, *12*, 5369.
26. Figueroa-Gerstenmaier, S.; Daniel, C.; Milano, G.; Vitillo, J. G.; Zavorotynska, O.; Spoto, G.; Guerra, G. *Macromolecules* **2010**, *43*, 8594.
27. Albunia, A. R.; Rizzo, P.; Ianniello, G.; Rufolo, C.; Guerra, G. *J. Polym. Sci. Pol. Phys.* **2014**, *52*, 657.
28. Burg, S. P.; Burg, E. A. *Science* **1965**, *148*, 1190.
29. Albunia, A. R.; Musto, P.; Guerra, G. *Polymer* **2006**, *47*, 234.
30. Wilchinsky, Z. W. In Advances in X-Ray Analysis; Mueller, W. M., Fay, M., Eds.; Plenum Press: New York, **1963**; Vol. *6*, p 231.
31. Alexander, L. E. In X-Ray Diffraction Methods in Polymer Science;, Krieger, R. E., Eds; Hintington: New York, **1979**, Chapter 4, p 198.
32. Robertson, G. L. In Food Packaging: Principles and Practice; 3rd ed.; CRC Press: New York, **1993**.
33. Torres, J. F.; Civalleri, B.; Meyer, A.; Musto, P.; Albunia, A. R.; Rizzo, P.; Guerra, G. *J. Phys. Chem. B* **2009**, *113*, 5059.
34. Albunia, A. R.; Rizzo, P.; Guerra, G. *Chem. Mat.* **2009**, *21*, 3370.
35. Larobina, D.; Sanguigno, L.; Venditto, V.; Guerra, G.; Mensitieri, G. *Polymer* **2004**, *45*, 429.
36. Kauffman, K. L.; Culp, J. T.; Goodman, A.; Matranga, C. *J. Phys. Chem. C* **2011**, *115*, 1857.
37. Milano, G.; Guerra, G.; Müller-Plathe, F. *Chem. Mat.* **2002**, *14*, 2977.
38. Venditto, V.; Girolamo Del Mauro, A. D.; Mensitieri, G.; Milano, G.; Musto, P.; Rizzo, P.; Guerra, G. *Chem. Mat.* **2006**, *18*, 2205.
39. Albunia, A. R.; Rizzo, P.; Guerra, G. *Polymer* **2013**, *54*, 1671.